P5.15 FREQUENCY DIVERSITY WIDEBAND WAVEORMS FOR DUAL-POLARIZATION WEATHER RADARS

Nitin Bharadwaj* and V. Chandrasekar
Colorado State University, Fort Collins, Colorado.

1 INTRODUCTION

Weather radar systems using solid-state transmitters are becoming increasingly viable. The transition from traditional high powered transmitters to solid-state transmitter is also useful to realize a network of low cost electronically steered X-band radars. However, solid-state transmitters have low peak powers which degrades the sensitivity of the radar if used in a conventional way with narrow transmit pulse. Sensitivity requirements with low peak power transmitters necessitates the use of pulse compression waveforms. Pulse compression radars transmit long wideband pulses to achieve adequate sensitivity and range resolution. Pulse compression has been in use with hard target radars for several decades and significant advances have been made in the technology and implementation (Cook and Bernfeld, 1993; Skolnik, 1990). Pulse compression techniques for non-weather radar systems are well documented in literature (Skolnik, 1990; Peebles, 1998). Their applicability to weather radar, however, is relatively rare. Typically weather radar targets are extended volume scatterers and range side-lobes are a major source of error for quantitative applications (Mudukutore et al., 1998). Mismatch filtering techniques to improve the range side-lobes have been studied, keeping in mind the applicability to weather radar.

Although pulse compression waveforms provide adequate sensitivity they have a major drawback in providing coverage at close range. Pulse compression waveforms suffer from blind zone that occur because the receiver does not receive any signal while the long pulse is being transmitted. The transmission of long pulses is necessary to achieve adequate sensitivity but results in blind ranges. Radars using pulse compression waveforms overcome blind range problem by staggering short and long pulses. The long pulse provides adequate sensitivity at farther ranges and short pulse provides coverage in the blind range region. However, alternating between long and short pulses reduces maximum unambiguous velocity. A pulse train of short pulse followed by a pulse train of long pulses can be used to provide adequate sensitivity and provide coverage in the blind range region. However, such a pulsing scheme will increase the dwell time resulting in slower scan speed.

In this paper a class of frequency diversity wideband waveforms are presented to mitigate low sensitivity of solid-state transmitters and also mitigate the blind zone problem associated with pulse compression. The proposed waveform is designed and implemented for a dual-polarization X-band radar operating in Simultaneous Transmit & Receive (STAR) mode. Frequency diversity is viable because a solid-state transmitters can achieve a much wider bandwidth with acceptable efficiency. The proliferation of low cost advanced digital processors, as well as the advances in digital transmitter control technology and low-power solid state transmitter technology makes the class of frequency diversity wideband waveforms viable for implementation. Some of the major considerations that needs to be taken into account for weather radars using solid-state transmitters is described in George et al. (2008).

2 PULSE COMPRESSION WAVEFORMS

A basic pulse compression waveform consists of a coding signal that modulates the transmitted pulse. Phase and frequency modulation have been widely used for pulse compression applications. For a pulse compression waveform the complex envelope of the transmitted wideband pulse is given by

$$g(t) = u(t) \exp\left\{ j2\pi \int_{-T/2}^{t} f(\tau)\, d\tau \right\} \qquad (1)$$

where $u(t)$ and T are the envelope, length of the transmitted pulse respectively and $g(t)$ is the complex envelope of the transmitted pulse. The pulse compression waveform describes $f(t)$. The matched filter which maximizes the signal-to-noise ratio is obtained as $g^*(-t)$ where $*$ indicates complex conjugate. The matched filter is completely determined by the complex envelope of the transmit pulse.

The range side lobes of a pulse compression waveform can be reduced by using a mismatch filter. The mismatch filters are obtained by using standard window functions and least-squares filters. Mismatch filters obtained from least-squares minimization have been

*Corresponding author address: Nitin Bharadwaj, 1373 Campus Delivery, Colorado State University, Fort Collins, Co 80523-1373.Email: nitin@engr.colostate.edu

known to provide good performance for some pulse compression waveforms. Ackroyd and Ghani (1973) proposed an inverse filter based on Wiener-Hopf equations and Mudukutore et al. (1998) evaluated the applicability of inverse filter using Barker codes for weather radars. Further, in Baden and Cohen (1990), an optimal Integrated Sidelobe Level (ISL) filter that minimized the ISL in the least squares sense was proposed (min ISL filter). The FIR filter coefficients of the mismatch compression filters are designed to minimize the ISL. The comparison of window based mismatch filter and minimum ISL filter is presented by Bharadwaj et al. (2008).

3 PULSE COMPRESSION WAVEFORMS FOR VOLUME TARGETS

In this section we describe the resolution and receiver bandwidth of pulse compression waveform. The effect of the side lobe levels on the estimated Doppler spectral moments for volume targets has been studied (Mudukutore et al., 1998; Bharadwaj et al., 2008). The impact of system phase noise and chirp bandwidth on the side lobe levels are described by Bharadwaj et al. (2008).

3.1 Range Resolution

In a traditional pulsed Doppler weather radar the range resolution is determined by the transmitted pulse width. However, the range resolution with a pulse compression waveforms is determined by the chirp bandwidth B and compression filter. In a matched filtered signal the range resolution is $c/2B$ where c is the speed of light. The range resolution with a pulse compression waveform can be obtained by simulating a point target and calculating the effective pulse width after the compression (Peebles, 1998). Figure 1 shows the range resolution using a minimum ISL filter.

3.2 Receiver Bandwidth

The spectrum of the transmitted pulse with frequency modulated pulse compression waveform is shown in Fig. 2(a) along with the filter characteristics of the minimum ISL filter and 80 dB Chebyshev window mismatch filter. It can be observed that the minimum ISL filter retains most of the frequency components while the 80 dB Chebyshev window filter has a narrower bandwidth. The bandwidth of the receiver is finite and this finite bandwidth causes a loss in received power because some of the spectral components of the received signal will be filtered out. It is important to have a filter which does not have a large finite bandwidth loss (ℓ_r). The finite bandwidth loss must be taken into account while estimating a calibrated reflectivity factor(Z_h). Table 1 lists the finite bandwidth loss for various compression filters applied to the pulse compression waveform.

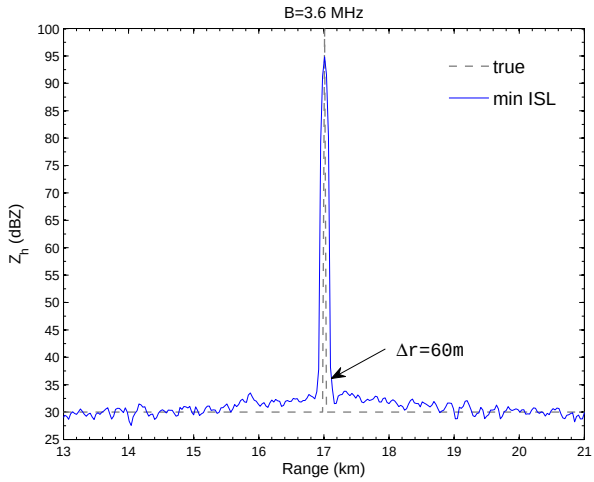

Figure 1: Range resolution using minimum ISL filter for Pulse compression waveform using $B = 3.6\ MHz$ and base-band sampling frequency $f_s = 5\ MHz$.

Table 1: Finite bandwidth filter loss for frequency diversity pulse compression waveform, $B = 3.6\ MHz$

Filter	$T = 20\ \mu s$ Filter loss (ℓ_r)	$T = 40\ \mu s$ Filter loss (ℓ_r)
min ISL	2.49 dB	1.83 dB
Hamming	3.47 dB	3.71 dB
Hann	3.70 dB	3.92 dB
Chebyshev 80 dB	4.65 dB	4.88 dB

4 FREQUENCY DIVERSITY WIDEBAND WAVEFORMS

The peak power of solid-state transmitters are generally low when compared to high powered transmitters such as Klystrons, Traveling Wave Tubes (TWT) and magnetrons. Traditional weather radars transmit short pulses with very high peak power to provide measurements with good sensitivity and range resolution. Weather radars using solid-state transmitters can not provide observations with adequate sensitivity by transmitting short pulses. To alleviate the problem of low sensitivity with solid-state transmitter based radars longer pulses must be transmitted. The inherent problem in the transmission of long pulses is the presence of blind ranges closer to the radar.

Blind ranges occurs because the back scattered signal from particles closer to the radar cannot be observed while the antenna is being used for transmission and this blind range corresponds to the duration of the long pulse. Therefore, a short pulse must be used to

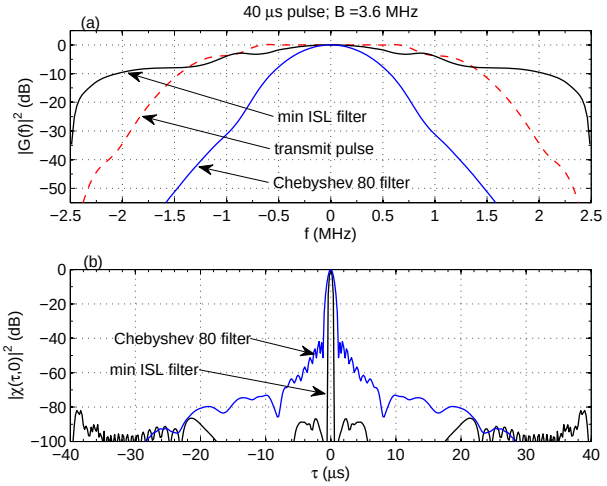

Figure 2: (a) Spectrum of transmit pulse and compression filter characteristics (b) Comparison of ambiguity function with 80 dB Chebyshev window filter and minimum ISL filter. The Pulse compression waveform has a nonlinear chirp of $B = 3.6MHz, T = 40\mu s$ pulse length, and base-band sampling frequency $f_s = 5\ MHz$.

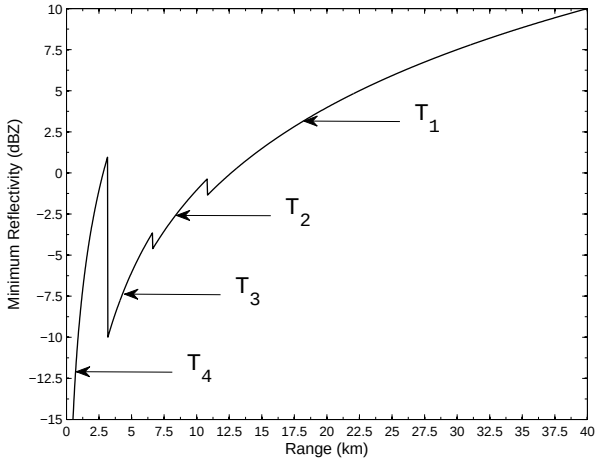

Figure 3: Minimum detectable reflectivity of a sensitivity mapped frequency diversity waveform.

provide coverage closer to the radar. However, the short pulse does not provide good sensitivity for the entire blind range caused by the longest pulse. Therefore, the sensitivity requirement must be mapped into a combination of sub-pulses as shown in Fig. 3. A class of waveforms as shown in Fig. 3 can be obtained by mapping the sensitivity to the generalized transmit waveform. For a generalized transmit-waveform, the complex envelope is composed of a sum of many components with varying sub-pulse widths. Each of the long pulse components are designed with pulse compression waveform using higher bandwidths to provide acceptable range resolution and adequate sensitivity.

In order to be able to avoid contamination of echoes from these individual components from the various ranges, the receiver must be able to separate the received signals corresponding to each component and this is accomplished by frequency diversity. In principle frequency diversity can be used to separate received signals from the short and long pulse components if the long and short pulses are separated in frequency. Ideally, both short and long pulses are transmitted simultaneously by using frequency diversity, however, intermodulation distortion in the saturated transmitter would introduce large amounts of spurious signals. The short pulse and long pulses at different center frequencies are multiplexed in time to form a frequency diversity wideband waveform. By design guidelines the first component is the longest pulse with the largest blind range and the last component is the shortest with minimal blind range. The final transmit waveform is subsequently obtained by mapping the operational and hardware requirements.

For example, the envelope of a frequency diversity wideband waveform with three components is shown in Fig. 4 (a). The frequency diversity wideband waveform shown in Fig. 4 consist of two long pulses and a short pulse. The time-frequency plot of this three component frequency diversity wideband waveform is shown in Fig. 4 (b) and it can clearly seen that the three components are orthogonal in time and frequency. The three components can be separated in the receiver because the individual waveform components are mutually orthogonal to each other in frequency domain. Such a class of frequency diversity wideband waveforms provide adequate sensitivity and spatial coverage to make solid-state transmitters viable to weather radar applications.

In order to ascertain the feasibility of the frequency diversity pulse compression waveform in a more realistic meteorological phenomenon a simulation based on observations from operational radars is performed. The data from from CSU-CHILL radar and X-band polarimetric radars deployed by Center for Collaborative Adaptive Sensing of the Atmosphere (CASA) is used as inputs for the simulations. A frequency diversity waveform consisting of three components is used to demonstrate the frequency diversity waveform. The pulse widths of the three components are $T_1 = 40\ \mu s$, $T_2 = 20\ \mu s$ and $T_3 = 1\ \mu s$. The waveform for each component using pulse compression is obtained for a $B = 3.6\ MHz$ chirp operating at a base band sampling frequency of $f_s = 5\ MHz$. The minimum ISL filter is chosen as the compression filter. The use of frequency diversity enables the mitigation of blind range. The measurements from the three frequencies are combined to provide observations without any blind range and adequate sensitivity.

A precipitation event with a well defined bright band

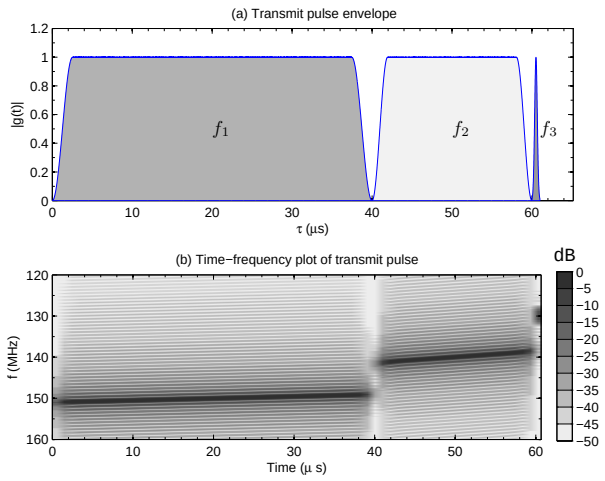

Figure 4: Time-frequency plot of the frequency diversity pulse compression waveform (a) Transmit pulse envelope (b) Time frequency plot.

was observed by CSU-CHILL radar on Jun 07, 2003 at 02:15:01 UTC. This bright band data set was used to simulate the received signal for a frequency diversity pulse compression waveform transmitted using a 100 W solid-state power amplifier. The simulations are carried out at three different frequencies whose center frequencies are separated by 10 MHz. A phase noise of 0.5 degree was added to the transmit waveform. The simulations were performed with $N = 64$ pulses at a PRF of 2 kHz. The characteristics of the solid-state radar used in the simulations is shown in Table 2. The calibration was done based on the radar constant for each component of the transmit waveform. The true bright band observations are shown in Fig. 5(a) which was obtained from a 500 kW peak-power radar. The reflectivity obtained by combining the observations from the three components of the transmit pulse is shown in Fig. 5(b). A comparison of the true reflectivity and that obtained from pulse compression agree well.

The observations made by the CASA radar at Chickasha on Mar 10, 2009 at 04:14:19 UTC and the results obtained with the frequency diversity pulse compression waveform are shown in Fig. 6 and 7. The precipitation event shown in Fig. 6 has weaker echoes close to the radar from azimuth of 240° to 330° and very strong reflectivities in the ranges covered by the longest pulse $T_1 = 40\ \mu s$ (azimuth 330° to 20°). The results obtained for the frequency diversity pulse compression waveform are combined from the three frequencies such that there is no blind range in the data and there is spatial continuity along range. This is particularly necessary for ϕ_{dp} because the system differential phase shift at the three different frequencies can lead to discontinuity in the range profiles of ϕ_{dp}. The reflectivity observed with the frequency diversity pulse compression is shown in Fig. 6(a) and it can be seen that they match very well with the input reflectivity. The reflectivity close to the radar is obtained from the short pulse while the weaker echoes farther away from the radar are obtained from the long pulses.

The observation of Z_{dr} from the frequency diversity pulse compression waveform is also in good agreement with the input Z_{dr} as shown in Fig. 6(b). The observed ϕ_{dp} and ρ_{hv} from the frequency diversity pulse compression waveform is compared with the input ϕ_{dp} and ρ_{hv} respectively and are shown in 7 (a) and (b) respectively. The increase in ϕ_{dp} along range (which indicates attenuation) in areas of significant precipitation is in good agreement between the input ϕ_{dp} distribution and the ϕ_{dp} distribution obtained from the pulse compression waveform. The retrieval of ϕ_{dp} is critical for attenuation correction algorithms. Similar simulation were carried out with other data sets (not shown) based on observations made by the CASA radar under identical set up. The simulations provided results comparable to the Chickasha results.

5 Summary

Waveforms for radar using solid-state transmitters are very important for achieving adequate sensitivity and coverage. A frequency diversity waveform using pulse compression was proposed for solid-state radars. A frequency diversity pulse compression waveform was simulated based on actual observations from CSU-CHILL radar at S-band and the CASA IP1 radars at X-band. A comparison of CSU-CHILL radar and CASA IP1 observations with the simulated X-band observation using frequency diversity pulse compression waveform indicates that frequency diversity pulse compression waveform does provide adequate sensitivity and coverage without blind range. The frequency diversity pulse compression waveform provided acceptable results in providing adequate sensitivity, minimizing range side lobes and mitigating blind range. Based on analysis performed on realistic simulations using CSU-CHILL radar data and CASA IP1 data the frequency diversity pulse compression waveform is suggested for polarimetric pulsed Doppler weather radars using solid-state transmitters.

6 ACKNOWLEDGEMENT

This work was supported by Colorado State University and the National Science Foundation under NSF Award Number 0313747.

Table 2: Solid-state radar characteristics used in simulations

Transmitter	
Type	Solid-state
Center frequency	9400 $\pm$ 100 MHz
Peak power output	100 W (per polarization channel)
Pulse width	maximum 70 μs
Polarization	Dual linear, Horizontal and Vertical
Max. Duty Cycle	15%
Antenna and Pedestal	
Type (diameter)	Parabolic reflector (2.4 m)
3-dB Beam width	1°
Gain	43.0 dB
Receiver	
Type	Dual-channel digital
Bandwidth	5 MHz (before compression filter)
Noise figure	4.0 dB
Sampling rate	5 MHz (baseband)

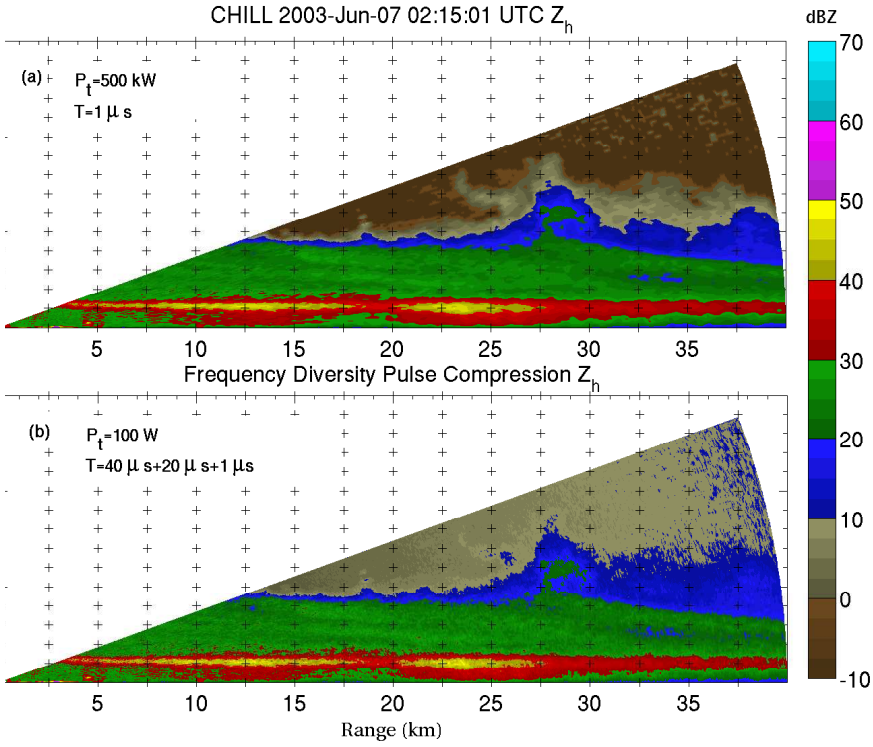

Figure 5: Simulation of frequency diversity pulse compression waveform for an X-band radar. (a) Observed reflectivity field from CSU-CHILL radar on Jun 07, 2003 at 02:15:01 UTC (b) The retrieved reflectivity from a frequency diversity pulse compression waveform.

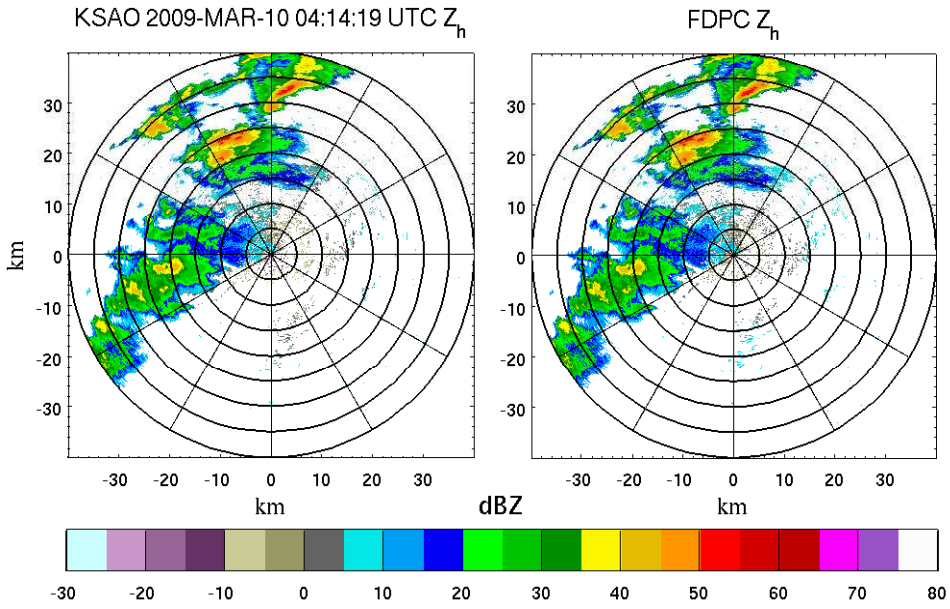

(a)

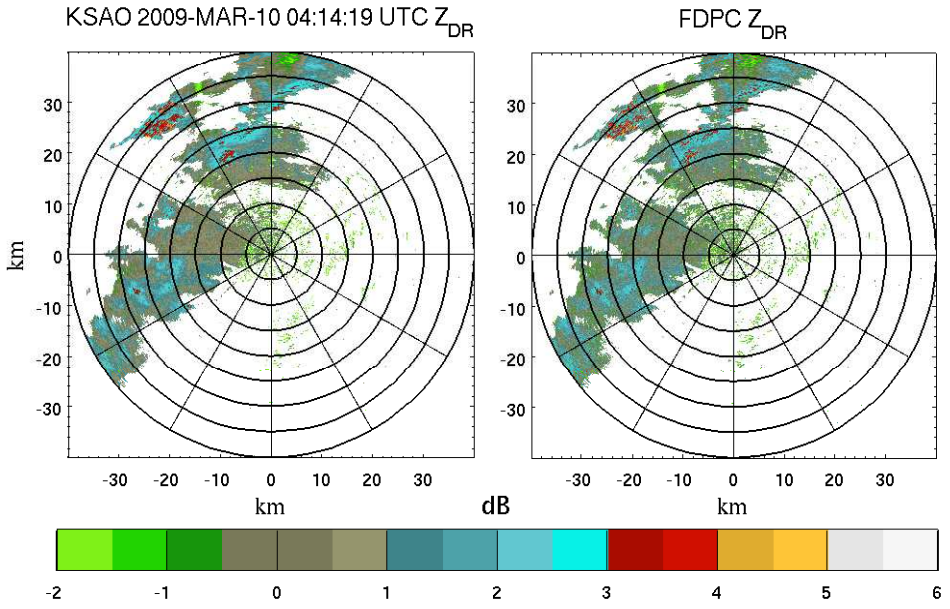

(b)

Figure 6: PPI plots of frequency diversity pulse compression waveform compared with the input data. The simulation is based on observation made with CASA IP1 radar at Chickasha on Mar 10, 2009 at 01:14:19 UTC. (a) Reflectivity (b) Z_{dr}.

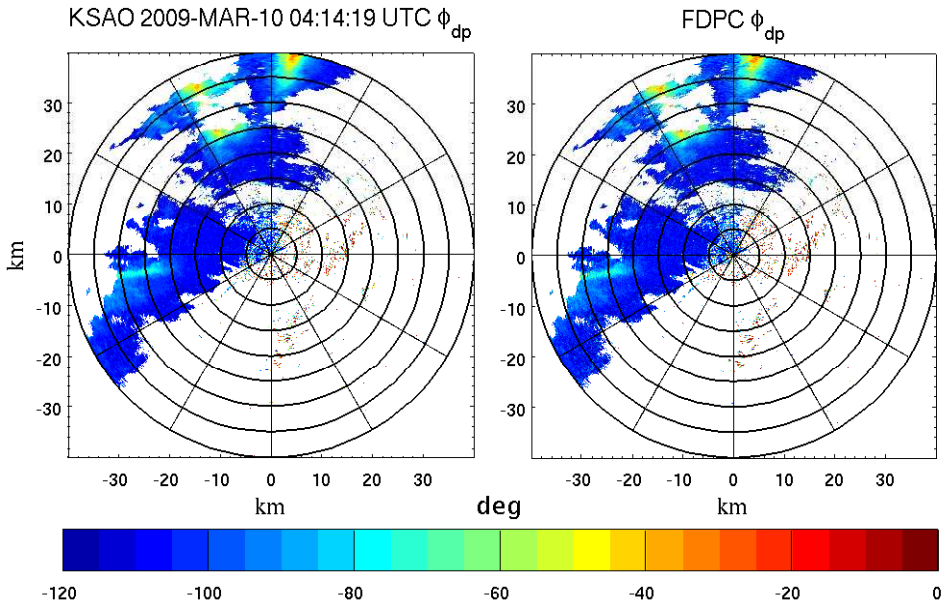

(a)

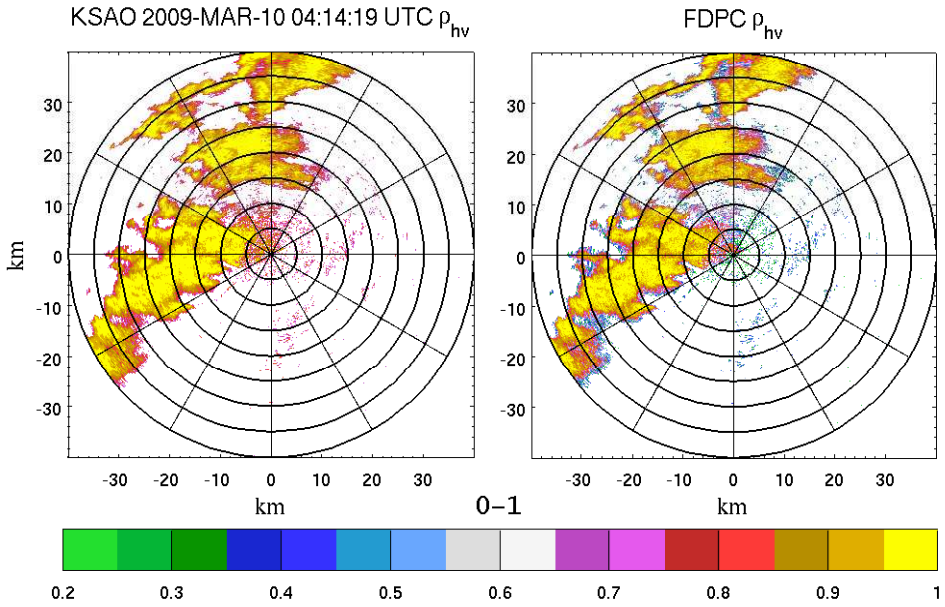

(b)

Figure 7: PPI plots of frequency diversity pulse compression waveform compared with the input data. The simulation is based on observation made with CASA IP1 radar at Chickasha on Mar 10, 2009 at 01:14:19 UTC. (a) ϕ_{dp} (b) ρ_{hv}.

References

Ackroyd, M. and F. Ghani, 1973: Optimum mismatched filters for sidelobe suppression. *Aerospace and Electronic Systems, IEEE Transactions on*, **AES-9**, 214–218.

Baden, J. and M. Cohen, 1990: Optimal peak sidelobe filters for biphase pulse compression. *Radar Conference, 1990., Record of the IEEE 1990 International*, IEEE, 249–252.

Bharadwaj, N., K. V. Mishra, and V. Chandrasekar, 2008: Waveform considerations for dual-polarization doppler weather radar with solid-state transmitters. *Geoscience and Remote Sensing Symposium, 2009. IGARSS 2009. IEEE International*, Cape Town,South Africa.

Chandrasekar, V., V. N. Bringi, and P. J. Brockwell, 1986: Statistical properties of dual-polarized radar signals. *23rd Conf. on Radar Meteorology*, Amer. Meteor. Soc., Snowmass,CO, 193–196.

Cook, C. E. and M. Bernfeld, 1993: *Radar Signals: An Introduction to Theory and Application*. Artech House, 552 pp.

George, J., N. Bharadwaj, and V. Chandrasekar, 2008: Pulse compression for weather radars. CDROM.

Mudukutore, A. S., V. Chandrasekar, and R. J. Keeler, 1998: Pulse compression for weather radars. *IEEE Trans. Geoscience and Remote Sensing.*, **36**, 125–142.

Peebles, P. Z., 1998: *Radar Principles*. Wiley-Interscience, 794 pp.

Skolnik, M. I., 1990: *Radar Handbook*. McGraw-Hill Professional, second edition, 1200 pp.